Structural Engineering and Mechanics, *Vol. 60, No. 4 (2016) 693-705*
DOI: http://dx.doi.org/10.12989/sem.2016.60.4.693

Interfacial stresses in RC beam bonded with a functionally graded material plate

Tahar Hassaine Daouadji*[1,2], Abdebasset Chedad[1,2] and Belkacem Adim[1,2]

[1]*Département de Génie Civil, Université Ibn Khaldoun Tiaret, BP 78 Zaaroura, 14000 Tiaret, Algérie*
[2]*Laboratoire de Géomatique et Développement Durable, Université Ibn Khaldoun de Tiaret, Algérie*

(Received June 18, 2016, Revised September 21, 2016, Accepted September 24, 2016)

Abstract. Functionally graded material (FGM) plates can be bonded to the soffit of a beam as a means of retrofitting the RC beam. In such plated beams, tensile forces develop in the bonded plate and these have to be transferred to the original beam via interfacial shear and normal stresses. In this paper, an interfacial stress analysis is presented for simply supported concrete beam bonded with a functionally graded material FGM plate. This new solution is intended for application to beams made of all kinds of materials bonded with a thin plate, while all existing solutions have been developed focusing on the strengthening of reinforced concrete beams, which allowed the omission of certain terms. It is shown that both the normal and shear stresses at the interface are influenced by the material and geometry parameters of the composite beam. This research is helpful for the understanding on mechanical behavior of the interface and design of the FGM-RC hybrid structures.

Keywords: RC beam; interfacial stresses; strengthening; functionally graded material plate

1. Introduction

The concept of functionally graded materials FGM were the first introduced in 1984 by a group of material scientists in Japan, as ultrahigh temperature resistant materials for aircraft, space vehicles and other engineering applications. Functionally graded materials are new composite materials in which the micro-structural details are spatially varied through non-uniform distribution of the reinforcement phase. The composite plate to upgrade structures and, in particular, to extend the lives of reinforced concrete beams has wide applications. One of the main aspects of the bonded strengthening technology is the stress analysis of the reinforced structure. In particular, reliable evaluation of the adhesive shear stress and of the stress in the CFRP plates is mandatory in order to predict the beam's failure load. Recently, the authors conducted a numerical study on the static behaviour of RC beams strengthened with composites in different directions (Tounsi 2006, Benyoucef 2006, Roberts 1989, Rabahi, Hassaine Daouadji *et al.* 2015, Hassaine Daouadji, Rabahi *et al.* 2016, Smith and Teng 2001, Shen 2001, Yang 2007, Bouakaz 2014, El Mahi 2014, Guenaneche 2014, Krour 2014, Touati 2015, Zidani 2015, yang 2010). Numerical examples and a parametric study are presented to illustrate the governing parameters

*Corresponding author, Professor, E-mail: daouadjitahar@gmail.com

http://www.techno-press.org/?journal=sem&subpage=8 ISSN: 1225-4568 (Print), 1598-6217 (Online)

that control the stress concentrations at the edge of the FRP strip. Finally, the results of these investigations show that the interface bond-stresses are non-uniformly distributed along the reinforced boundaries. It is believed that the present results will be of interest to civil and structural engineers and researchers.

The objective of this analytical study is to improve the famous method developed by Tounsi (2006) by incorporating with the adherend shear deformations. Indeed, it is reasonable to assume that the shear stresses, which develop in the adhesive, are continuous across the adhesive-adherend interface. The importance of including shear-lag effect of the adherents was shown by Tounsi (2006). The obtained results are in good agreement with those of numerical results. The presented method predicts also, maximum values in cut-off section, but comparatively, the computed interfacial stresses are considerably smaller than those obtained by other models which neglect adherent shear deformations. Hence, the adopted improved model describes better actual response of the FGM-RC hybrid beams and permits the evaluation of the interfacial stresses, the knowledge of which is very important in the design of such structures. In this paper, the details of the interfacial shear and normal stress are analyzed by the theoretical method. The effects of the material and geometry parameters on the interface stresses are considered and compared with that resulting from literature. Finally, some concluding remarks are summarized in conclusion. It is believed that the present results will be of interest to civil and structural engineers and researchers.

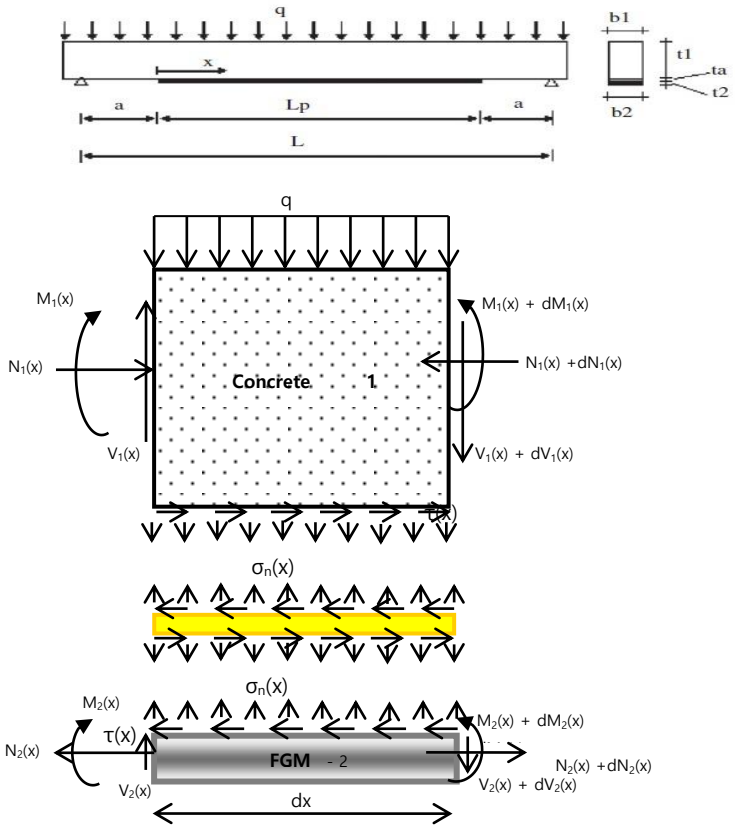

Fig. 1 Simply supported RC beam strengthened with bonded FGM plate

2. Method of solution

2.1 Assumptions

The present analysis takes into consideration the transverse shear stress and strain in the beam and the plate but ignores the transverse normal stress in them. One of the analytical approach proposed by Hassaine Daouadji, Rabahi *et al.* (2016) for concrete beam strengthened with a bonded FGM Plate (Fig. 1) was used in order to compare it with a finite element analysis. The analytical approach (Hassaine Daouadji, Rabahi *et al.* 2016) is based on the following assumptions:

- Elastic stress strain relationship for concrete, FGM and adhesive;
- There is a perfect bond between the composite plate and the beam;
- The adhesive is assumed to only play a role in transferring the stresses from the concrete to the composite plate reinforcement;
- The stresses in the adhesive layer do not change through the direction of the thickness.

Since the functionally graded materials is an orthotropic material. In analytical study (Hassaine Daouadji, Rabahi *et al*. 2016), the classical plate theory is used to determine the stress and strain behaviours of the externally bonded composite plate in order to investigate the whole mechanical performance of the composite - strengthened structure.

2.2 Properties of the FGM constituent materials

The functionally graded material (FGM) can be produced by continuously varying the constituents of multi-phase materials in a predetermined profile. The most distinct features of an FGM are the non-uniform microstructures with continuously graded macro properties. An FGM can be defined by the variation in the volume fractions (Albasyouni 2015, Belabed 2014, Bensatallah 2016, Bouaza 2015, Boumia 2014). Most researchers use the power-law function or exponential function to describe the volume fractions. However, only a few studies used sigmoid function to describe the volume fractions. Therefore, FGM beams with sigmoid function will be considered in this paper in detail. Consider an elastic FGM plate of uniform thickness $\boldsymbol{h}$, which is made of a ceramic and metal, is considered in this study. The material properties, Young's modulus and the Poisson's ratio, on the upper and lower surfaces are different but are preassigned according to the performance demands. However, the Young's modulus and the Poisson's ratio of the beams vary continuously only in the thickness direction (z-axis) i.e., $E=E(z)$, $\upsilon=\upsilon(z)$. Hassaine Daouadji (2013) indicated that the effect of Poisson's ratio on the deformation is much less than that of Young's modulus. Thus, Poisson's ratio of the plate is assumed to be constant. However, the Young's modules in the thickness direction of the FGM beams vary with power-law functions (P-FGM) or with exponential functions (E-FGM) (Bourada 2015, Bourada 2015, Bouramana 2016, Zidour 2014).

The material properties of FGM plates are assumed to vary continuously through the thickness. Three homogenization methods are deployable for the computation of the Young's modulus E(z) namely:

- The exponential distribution E-FGM,
- The power law distribution P-FGM,
- The Mori-Tanaka scheme.

For the exponential distribution E-FGM, the Young's modulus is given as Hassaine daouadji

(2013)

$$E(z) = E_2 . e^{\frac{1}{h}\ln(\frac{E_1}{E_2})(z+\frac{h}{2})} \tag{1}$$

where E_2 is the Young's modulus of the homogeneous plate; E_2 denote Young's modulus of the bottom (as metal) and top E_1 (as ceramic) surfaces of the FGM plate, respectively; E_2 is Young's modulus of the homogeneous plate; and p is a parameter that indicates the material variation through the plate thickness. For the power law distribution P-FGM, the Young's modulus is given as Hassaine daouadji (2013)

$$E(z) = E_2 + (E_1 - E_2)(\frac{z}{h} + \frac{1}{2})^p \tag{2a}$$

Consider an imperfect FGM with a porosity volume fraction, α (α<<1), distributed evenly among the metal and ceramic, the modified rule of mixture proposed by Wattanasakul pong and Ungbhakorn (2014), the Young's modulus E equations of the imperfect FGM beam can be expressed as

$$E(z) = E_2 + (E_1 - E_2)(\frac{z}{h} + \frac{1}{2})^P - (E_1 + E_2)\frac{\alpha}{2} \tag{2b}$$

For Mori-Tanaka scheme, the Young's modulus is given as (Mori and Tanaka 1973)

$$E(z) = E_2 + (E_1 - E_2)\frac{(\frac{z}{h} + \frac{1}{2})^p}{1 + (1 - (\frac{z}{h} + \frac{1}{2})^p)(\frac{E_1}{E_2} - 1)\frac{1+\nu}{3-3\nu}} \tag{3}$$

The linear constitutive relations of a FG plate can be written as

$$\begin{Bmatrix} \sigma_x \\ \sigma_y \\ \tau_{yz} \\ \tau_{xz} \\ \tau_{xy} \end{Bmatrix} = \begin{bmatrix} Q_{11} & Q_{12} & 0 & 0 & 0 \\ Q_{12} & Q_{22} & 0 & 0 & 0 \\ 0 & 0 & Q_{44} & 0 & 0 \\ 0 & 0 & 0 & Q_{55} & 0 \\ 0 & 0 & 0 & 0 & Q_{66} \end{bmatrix} \begin{Bmatrix} \varepsilon_x \\ \varepsilon_y \\ \gamma_{yz} \\ \gamma_{xz} \\ \gamma_{xy} \end{Bmatrix} \tag{4}$$

where (σ_x, σ_y, τ_{xy}, τ_{yz}, τ_{yx}) and (ε_x, ε_y, γ_{xy}, γ_{yz}, γ_{yx}) are the stress and strain components, respectively .

The computation of the elastic constants Q_{ij} in the plane stress reduced elastic constants, defined as

$$Q_{11} = Q_{22} = \frac{E(z)}{1-\nu^2} \qquad Q_{12} = \frac{\nu\, E(z)}{1-\nu^2} \quad \text{and} \quad Q_{44} = Q_{55} = Q_{66} = \frac{E(z)}{2(1+\nu)} \tag{5}$$

where A_{ij}, D_{ij} are the plate stiffness, defined by

$$A_{ij} = \int_{-h/2}^{h/2} Q_{ij} dz \qquad D_{ij} = \int_{-h/2}^{h/2} Q_{ij} z^2 dz \tag{6}$$

where $A_{11}^{'}$, $D_{11}^{'}$ are defined as

$$A_{11}^{'} = \frac{A_{22}}{A_{11}A_{22} - A_{12}^2} \qquad D_{11}^{'} = \frac{D_{22}}{D_{11}D_{22} - D_{12}^2} \tag{7}$$

2.3 Shear stress distribution along the FGM - concrete interface

The governing differential equation for the interfacial shear stress (Hassaine Daouadji, Rabahi *et al.* 2016) is expressed as

$$\frac{d^2\tau(x)}{dx^2} - K_1\left(A_{11}^{'} + \frac{b_2}{E_1A_1} + \frac{(y_1+t_2/2)(y_1+t_a+t_2/2)}{E_1I_1D_{11}^{'}+b_2}b_2D_{11}^{'}\right)\tau(x) + K_1\left(\frac{(y_1+t_2/2)}{E_1I_1D_{11}^{'}+b_2}D_{11}^{'}\right)V_T(x) = 0 \quad (8)$$

Where

$$K_1 = \frac{1}{\left(\frac{t_a}{G_a} + \frac{t_1}{4G_1}\right)} \quad (9)$$

For simplicity, the general solutions presented below are limited to loading which is either concentrated or uniformly distributed over part or the whole span of the beam, or both. For such loading, $d^2V_T(x)/dx^2 = 0$, and the general solution to Eq. (8) is given by

$$\tau(x) = B_1\cosh(\lambda x) + B_2\sinh(\lambda x) + m_1V_T(x) \quad (10)$$

Where

$$\lambda^2 = K_1\left(A_{11}^{'} + \frac{b_2}{E_1A_1} + \frac{(y_1+t_2/2)(y_1+t_a+t_2/2)}{E_1I_1D_{11}^{'}+b_2}b_2D_{11}^{'}\right) \quad (11)$$

$$m_1 = \frac{K_1}{\lambda^2}\left(\frac{(y_1+t_2/2)}{E_1I_1D_{11}^{'}+b_2}D_{11}^{'}\right) \quad (12)$$

And B_1 and B_2 are constant coefficients determined from the boundary conditions. In the present study, a simply supported beam has been investigated which is subjected to a uniformly distributed load (Fig. 1). The interfacial shear stress for this uniformly distributed load at any point is written as (Hassaine Daouadji, Rabahi *et al.* 2016)

$$\tau(x) = \left[\frac{m_2a}{2}(L-a) - m_1\right]\frac{qe^{-\lambda x}}{\lambda} + m_1q\left(\frac{L}{2} - a - x\right) \qquad 0 \le x \le L_P \quad (13)$$

Where q is the uniformly distributed load and x; a; L and L_p are defined in Fig. 1.

2.4 Normal stress distribution along the FGM - concrete interface

The following governing differential equation for the interfacial normal stress (Hassaine Daouadji, Rabahi *et al.* 2016)

$$\frac{d^4\sigma_n(x)}{dx^4} + K_n\left(D_{11}^{'} + \frac{b_2}{E_1I_1}\right)\sigma_n(x) - K_n\left(D_{11}^{'}\frac{t_2}{2} - \frac{y_1b_2}{E_1I_1}\right)\frac{d\tau(x)}{dx} + \frac{qK_n}{E_1I_1} = 0 \quad (14)$$

The general solution to this fourth-order differential equation is

$$\sigma_n(x) = e^{-\beta x}\left[C_1\cos(\beta x) + C_2\sin(\beta x)\right] + e^{\beta x}\left[C_3\cos(\beta x) + C_4\sin(\beta x)\right] - n_1\frac{d\tau(x)}{dx} - n_2q \quad (15)$$

For large values of x it is assumed that the normal stress approaches zero and, as a result, C_3=

C_4= 0. The general solution therefore becomes

$$\sigma_n(x) = e^{-\beta x}[C_1 \cos(\beta x) + C_2 \sin(\beta x)] - n_1 \frac{d\tau(x)}{dx} - n_2 q \tag{16}$$

Where

$$\beta = \sqrt[4]{\frac{K_n}{4}\left(D_{11}^{'} + \frac{b_2}{E_1 I_1}\right)} \tag{17}$$

$$n_1 = \left(\frac{y_1 b_2 - D_{11}^{'} E_1 I_1 t_2 / 2}{D_{11}^{'} E_1 I_1 + b_2}\right) \quad n_2 = \frac{1}{D_{11}^{'} E_1 I_1 + b_2} \tag{18}$$

As is described by Hassaine Daouadji, Rabahi *et al.* (2016), the constants C_1 and C_2 in Eq. (16) are determined using the appropriate boundary conditions and they are written as follows

$$C_1 = \frac{K_n}{2\beta^3 E_1 I_1}[V_T(0) + \beta M_T(0)] - \frac{n_3}{2\beta^3}\tau(0) + \frac{n_1}{2\beta^3}\left(\frac{d^4\tau(0)}{dx^4} + \beta\frac{d^3\tau(0)}{dx^3}\right) \tag{19}$$

$$C_2 = -\frac{K_n}{2\beta^2 E_1 I_1} M_T(0) - \frac{n_1}{2\beta^2}\frac{d^3\tau(0)}{dx^3} \tag{20}$$

$$n_3 = b_2 K_n\left(\frac{y_1}{E_1 I_1} - \frac{D_{11}^{'} t_2}{2b_2}\right) \tag{21}$$

The above expressions for the constants C_1 and C_2 has been left in terms of the bending moment $M_T(0)$ and shear force $V_T(0)$ at the end of the soffit plate. With the constants C_1 and C_2 determined, the interfacial normal stress can then be found using Eq. (16).

3. Numerical verification and discussions

3.1 Comparison with approximate solutions

The present simple solution is compared, in this section, with some approximate solutions available in the literature. These include Smith and Teng (2001), Tounsi (2007), Hassaine Daouadji, Rabahi *et al*. (2016) solutions uniformly distributed loads. A comparison of the interfacial shear and normal stresses from the different existing closed-form solutions and the present solution is undertaken in this section. An undamaged beams bonded with CFRP, FGM and sandwich (P-FGM core) plate soffit plate is considered. The beam is simply supported and subjected to a uniformly distributed load. A summary of the geometric and material properties is given in Table 1. The results of the peak interfacial shear and normal stresses are given in Table 2 for the beams strengthened by bonding CFRP, FGM and sandwich (P-FGM core) plate. As it can be seen from the results, the peak interfacial stresses assessed by the present theory are smaller compared to those given by Smith and Teng (2001), Tounsi (2007), Hassaine Daouadji, Rabahi *et al.* (2016) solutions. This implies that adherend shear deformation is an important factor influencing the adhesive interfacial stresses distribution. Fig. 2 plots the interfacial shear and normal stresses near the plate end for the example RC beam bonded with a FGM plate for the uniformly distributed load case. Overall, the predictions of the different solutions agree closely

Table 1 Geometric and material properties

Component	Width (mm)	Depth (mm)	Young's modulus (MPa)	Poisson's ratio	Shear modulus (MPa)
RC beam	b_1 = 200	t_1=300	E_1 = 30 000	0.18	-
Adhesive layer RC beam	b_a = 200	t_a = 4	E_a = 3000	0.35	-
GFRP plate (bonded RC beam)	b_2 = 200	t_2= 4	E_2 = 50 000	0.28	G_{12} =5000
CFRP plate (bonded RC beam)	b_2 = 200	t_2= 4	E_2 = 140 000	0.28	G_{12} =5000
FGM (Al_2O_3) plate (bonded RC beam)	b_2 = 200	t_2= 4	E_2 = 380 000	0.3	G_{12} =5000
FGM (ZrO_2) plate (bonded RC beam)	b_2 = 200	t_2= 4	E_2 = 200 000	0.3	G_{12} =5000

Table 2 Comparison of peak interfacial shear and normal stresses (MPa): Uniformly Distributed Load- UDL

Model	Shear	Normal
Tounsi, Hassaine Daouadji *et al.* (2007) "RC beam with CFRP plate"	1.96203	1.1694
Smith and Teng (2001) "RC beam with CFRP plate"	3.8347	2.1012
Hassaine Daouadji, Rabahi *et al*. (2016) "RC beam with CFRP plate"	1.9982	1.1887
Present Model "RC beam with P-FGM plate" P-FGM = Al_2O_3 (P=2)	2.1573	1.1939
Present Model "RC beam with P-FGM plate" P-FGM = ZrO_2 (P=2)	1.7801	1.0945
Present Model "RC beam with E-FGM plate" E-FGM = Al_2O_3	2.2099	1.2151
Present Model "RC beam with E-FGM plate" E-FGM = ZrO_2	1.8449	1.1277
Present Model "RC beam with sandwich plate" Type A: Homogeneous face sheet and P-FGM core - (P-FGM=Al_2O_3 (P=2)	2.0807	1.2202
Present Model "RC beam with sandwich plate" Type B: Homogeneous face sheet and P-FGM core - (P-FGM= ZrO_2 (P=2)	1.7895	1.10466

with each other. The interfacial normal stress is seen to change sign at a short distance away from the plate end. The present analysis gives lower maximum interfacial shear and normal stresses than those predicted by Tounsi (2006), Hassaine Daouadji, Rabahi *et al.* (2016), indicating that the inclusion of adherend shear de formation effect in the beam and soffit plate leads to lower values of $\sigma_{\max}$ and $\sigma_{\max}$. However, the maximum interfacial shear and normal stresses given by Tounsi (2006), Hassaine Daouadji, Rabahi *et al*. (2016) methods are lower than the results computed by the present solution. This difference is due to the assumption used in the present theory which is in agreement with the beam theory. Hence, it is apparent that the adherend shear deformation reduces the interfacial stresses concentration and thus renders the adhesive shear distribution more uniform. The interfacial normal stress is seen to change sign at a short distance away from the plate end.

The results of the peak interfacial shear and normal stresses are given in Table 2 for the RC beam with a CFRP, FGM and sandwich soffit plate. Table 2 shows that, for the UDL case, the present solution gives results which generally agree better with those from Smith's and Teng (2001), Tounsi's (2007), Hassaine Daouadji's *et al.* (2016) solutions. The latter two again give similar results. In short, it may be concluded that all solutions are satisfactory for RC beams bonded with a thin plate as the rigidity of the soffit plate is small in comparison with that of the RC beam. Those solutions which consider the additional bending and shear deformations in the soffit plate due to the interfacial shear stresses give more accurate results. The present solution is

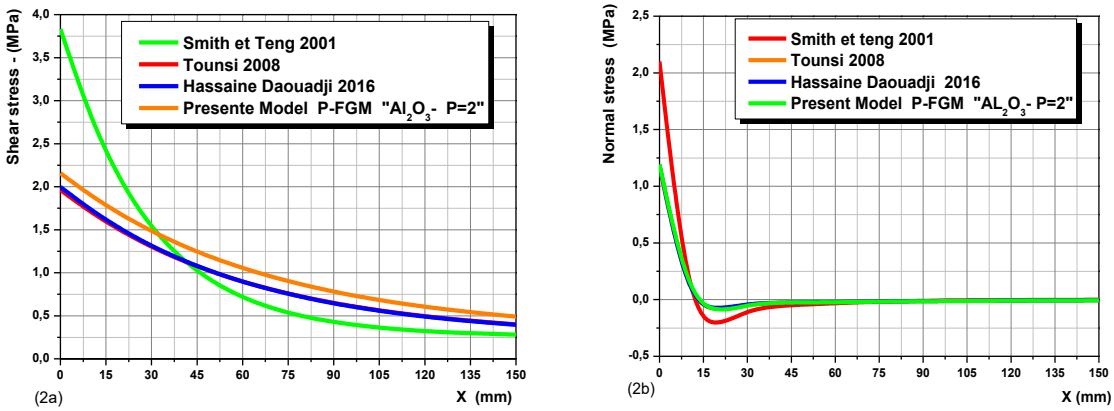

Fig. 2 Comparison of interfacial shear and normal stress for P-FMP plated RC beam with the analytical results: (a) Shear stress (b) Normal stress

Table 3 Comparison of peak interfacial shear and normal stresses: Effect of plate stiffness

Material		Shear stress	Normal stress
CFRP		1.9620	1.1694
GFRP		1.1943	0.8995
Steel		2.3326	1.2795
P-FGM - (P=2)	Al2 O3	2.1573	1.1939
	ZrO2	1.78010	1.09456
E-FGM	Al2 O3	2.20992	1.21514
	ZrO2	1.85491	1.12777
Mori Tanaka	Al2 O3	1.8685	1.68572
	ZrO2	1.0873	1.05495
Sandwich	Homogeneous face sheet and P-FGM core , P-FGM-Al2 O3	2.08073	1.22022
	Homogeneous face sheet and P-FGM core, P-FGM-ZrO2	1.78955	1.10466

the only solution which covers the uniformly distributed loads and considers this effect and the effects of other parameters.

3.2 Parametric studies

To better understand the behavior of bonded beam repairs, which will help engineers in optimizing their design parameters, the effects of several parameters were investigated. The material used for the present studies is an RC beam bonded with a FGM plate. The beams are simply supported and subjected to a uniformly distributed load. A summary of the geometric and material properties is given in Table 1. The span of the RC beam is 3000 mm, the distance from the support to the end of the plate is 300 mm and the uniformly distributed load is 50 kN/m.

Effect of plate stiffness on interfacial stress:

Table 4 Effect of plate stiffness on interfacial stresses in FGM strengthened RC beam

Material	P-FGM - Al_2O_3						
	Ceramic: $P = 0$	$P = 0,5$	$P = 2$	$P = 5$	$P = 10$	$P = 100$	Aluminum: $P = \infty$
Shear stress	2.9391	2.6158	2.1573	1.8398	1.6635	1.4420	1.4120
Normal stress	1.3972	1.3484	1.1939	1.0658	1.0064	0.9790	0.9855
Material	P-FGM - ZrO_2						
	Ceramic: $P = 0$	$P = 0,5$	$P = 2$	$P = 5$	$P = 10$	$P = 100$	Aluminum: $P = \infty$
Shear stress	2.29383	2.06355	1.78010	1.60980	1.52388	1.42472	1.41202
Normal stress	1.26050	1.20763	1.09456	1.01908	.99022	.98252	.98556
Material	E-FGM						
	$E_1/E_2 = 1$	$E_1/E_2 = 2$	$E_1/E_2 = 3$	$E_1/E_2 = 4$	$E_1/E_2 = 5$	$E_1/E_2 = 6$	$E_1/E_2 = 7$
Shear stress	1.41202	1.68595	1.87959	2.03286	2.16082	2.27106	2.36808
Normal stress	.98556	1.07861	1.13450	1.17403	1.20420	1.22828	1.24808
Material	FGM (Mori-tanaka) - Al_2O_3						
	Ceramic: $P = 0$	$P = 0,5$	$P = 2$	$P = 5$	$P = 10$	$P = 100$	Aluminum: $P = \infty$
Shear stress	2.93916	2.31342	1.86825	1.64729	1.54286	1.3367	1.41202
Normal stress	1.39722	1.25191	1.08783	1.01091	.98511	.97556	0.9582
Material	FGM (Mori-tanaka) ZrO_2						
	Ceramic: $P = 0$	$P = 0,5$	$P = 2$	$P = 5$	$P = 10$	$P = 100$	Aluminum: $P = \infty$
Shear stress	2.29383	1.95679	1.68572	1.55135	1.48886	1.3905	1.41202
Normal stress	1.26050	1.16785	1.05495	1.00168	0.98490	0.97556	0.9672
Material	Sandwich: Homogeneous face sheet and P-FGM core					P-FGM- Al_2O_3	
	Ceramic: $P = 0$	$P = 0,5$	$P = 2$	$P = 5$	$P = 10$	$P = 100$	Aluminum: $P = \infty$
Shear stress	2.74646	2.46101	2.08073	1.83430	1.70383	1.54723	1.52664
Normal stress	1.46241	1.38440	1.22022	1.10139	1.04413	0.99076	0.98592
Material	Sandwich: Homogeneous face sheet and P-FGM core					P-FGM- ZrO_2	
	Ceramic: $P = 0$	$P = 0,5$	$P = 2$	$P = 5$	$P = 10$	$P = 100$	Aluminum: $P = \infty$
Shear stress	2.19097	2.00645	1.78955	1.66507	1.60407	1.53532	1.52664
Normal stress	1.28005	1.21124	1.10466	1.04003	1.01188	0.98795	0.98592

Table 3 and 4 gives interfacial normal and shear stresses for the RC beam bonded with a CFRP, GFRP, steel and FGM plate, respectively, which demonstrates the effect of plate material properties on interfacial stresses. The length of the plate is Lp=2400 mm, and the thickness of the plate and the adhesive layer are both 4 mm. The results show that, as the plate material becomes softer (from FGM to steel, to CFRP and then GFRP), the interfacial stresses become smaller, as expected. This is because, under the same load, the tensile force developed in the plate is smaller, which leads to reduced interfacial stresses. The position of the peak interfacial shear stress moves closer to the free edge as the plate becomes less stiff.

Effect of plate stiffness on interfacial stress : Fig. 4 and Table 4 gives interfacial normal and shear stresses for the RC beam bonded with a FGM plate, respectively, which demonstrates the effect of plate material properties on interfacial stresses. The length of the plate is Lp=2400 mm, and the thickness of the plate and the adhesive layer are both 4mm. The results show that, as the

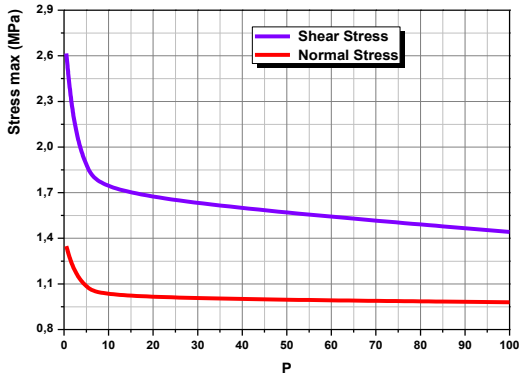

Fig. 3 Effect of degree of homogeneity on interfacial stresses in P-FGM (P=2) strengthened RC beam

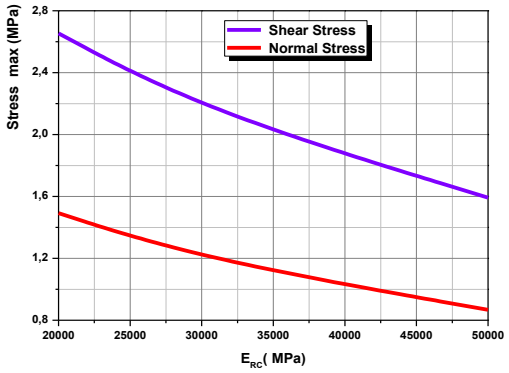

Fig. 4 Effect of plate stiffness on interfacial stresses in FGM strengthened RC beam

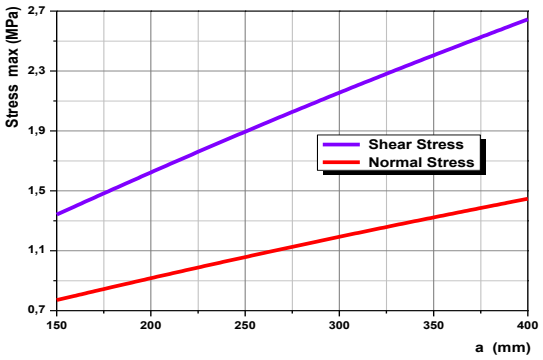

Fig. 5 Influence of length of unstrengthened region on edge stresses for RC beam with a bonded P-FGM soffit plate

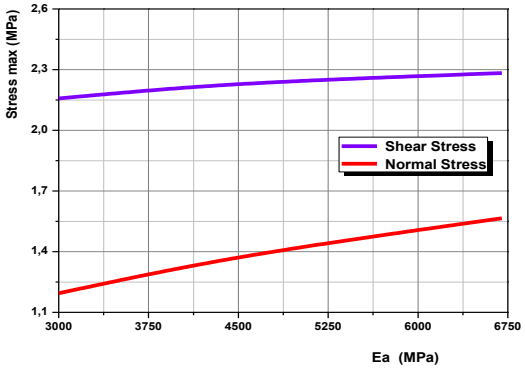

Fig. 6 Effect of adhesive moduli on interfacial stresses in P-FGM (P=2) strengthened RC beam

plate material becomes softer (from FGM- Al2 O3 to FGM - ZrO2 and then Sandwich with homogeneous face sheet and FGM core), the interfacial stresses become smaller, as expected. This is because, under the same load, the tensile force developed in the plate is smaller, which leads to reduced interfacial stresses. The position of the peak interfacial shear stress moves closer to the free edge as the plate becomes less stiff.

Effect of length of unstrengthened region a:

The influence of the length of the ordinary-beam region (the region between the support and the end of the composite strip on the edge stresses) appears in Fig 5. It is seen that, as the plate terminates further away from the supports, the interfacial stresses increase significantly. This result reveals that in any case of strengthening, including cases where retrofitting is required in a limited zone of maximum bending moments at midspan, it is recommended to extend the strengthening strip as possible to the lines.

***Effect of elasticity modulus of adhesive layer*:** The adhesive layer is a relatively soft,

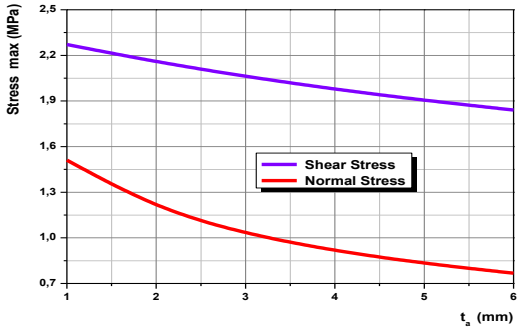

Fig. 7 Effect of adhesive layer thickness on edge shear stresses in P-FGM strengthened RC beam

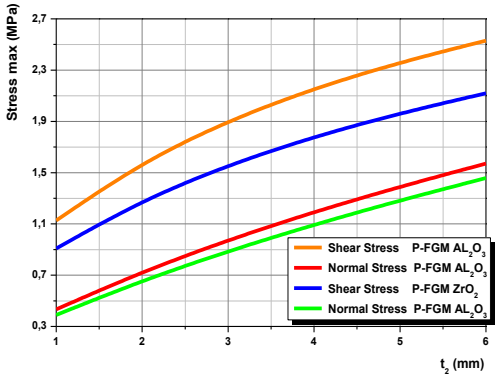

Fig. 8 Effect of plate thickness on interfacial stresses in P-FGM (*P*=2) strengthened RC beam

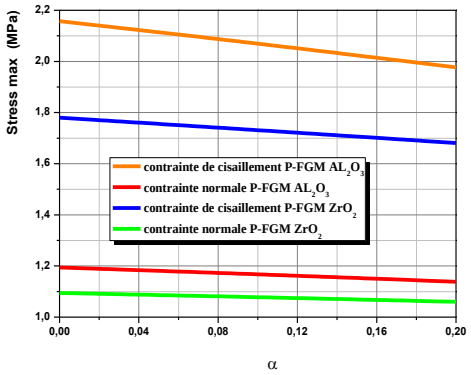

Fig. 9 Effect of porosity in P-FGM plate on interfacial stresses strengthened RC beam

isotropic material and has a smaller stiffness. The four sets of Young's moduli are considered here, which are 3, 4, 5 and 6.7 GPa. The Poisson's ratio of the adhesive is kept constant. The numerical results in fig. 6 show that the property of the adhesive hardly influences the level of the interfacial stresses, whether normal or shear stress, but the stress concentrations at the end of the plate increase as the Young's modulus of the adhesive increases.

Effect of adhesive layer thickness: Fig. 7 shows the effects of the thickness of the adhesive layer on the interfacial stresses. Increasing the thickness of the adhesive layer leads to a significant reduction in the peak interfacial stresses. Thus using thick adhesive layer, especially in the vicinity of the edge, is recommended. In addition, it can be shown that these stresses decrease during time, until they become almost constant after a very long time.

Effect of plate thickness and porosity: The thickness of the FRP plate is an important design variable in practice. Figs. 8 and 9 shows the effect of the thickness of the FRP plate on the interfacial stresses. Here, three values of the thickness, 2, 4 and 6 mm, are considered. It is shown that the level and concentration of interfacial stress are influenced considerably by the thickness of the FRP plate. The interfacial stresses increase as the thickness of FRP plate increases. Generally, the thickness of FRP plates used in practical engineering is small, compared with that of steel

plate. Therefore, the fact of the smaller interfacial stress level and concentration should be one of the advantages of retrofitting by FRP plate compared with a steel plate.

4. Conclusions

This paper has been concerned with the prediction of interfacial shear and normal stresses in reinforced concrete beams strengthened by externally bonded functionally graded FGM plate. Such interfacial stresses provide the basis for understanding debonding failures in such RC beams and for the development of suitable design rules. It is shown that the in homogeneities play an important role in interfacial stresses. The obtained solution could serve as a basis for establishing simplified FGM theories or as a benchmark result to assess other approximate methodologies. We can conclude that, This research is helpful for the understanding on mechanical behavior of the interface and design of the FGM-RC hybrid structures. The new solution is general in nature and may be applicable to all kinds of materials.

Acknowledgments

The authors thank the referees for their valuable comments.

References

Al-Basyouni, K.S., Tounsi, A. and Mahmoud, S.R. (2015), "Size dependent bending and vibration analysis of functionally graded micro beams based on modified couple stress theory and neutral surface position", *Compos. Struct*., **125**, 621-630.

Belabed, Z., Houari, M.S.A., Tounsi, A., Mahmoud, S.R. and Anwar Bég, O. (2014), "An efficient and simple higher order shear and normal deformation theory for functionally graded material (FGM) plates", *Compos. Part B*, **60**, 274-283.

Bensattalah, T., Hassaine Daouadji, T., Zidour, M., Tounsi, A. and Bedia, E.A.A. (2016), "Investigation of thermal and chirality effects on vibration of single-walled carbon anotubes embedded in a polymeric matrix using nonlocal elasticity theories", *Mech. Compos. Mater.*, **52**(4), 555-568.

Benyoucef, S., Tounsi, A., Meftah, S.A. and Adda Bedia, E.A. (2006), "Approximate analysis of the interfacial stress concentrations in FRP-RC hybrid beams", *Compos. Interf.*, **13**(7), 561-71.

Bouakaz, K., Hassaine Daouadji, T., Meftah, S.A., Ameur, M. and Adda Bedia, E.A. (2014), "A numerical analysis of steel beams strengthened with composite materials", *Mech. Compos. Mater*., **50**(4), 685-696.

Bouazza, M., Amara, K., Zidour, M., Tounsi, A. and Adda-Bedia, E.A. (2015), "Postbuckling analysis of nanobeams using trigonometric Shear deformation theory", *Appl. Sci. Report.*, **10**(2), 112-121.

Boumia, L., Zidour, M., Benzair, A. and Tounsi, A. (2014), "A Timoshenko beam model for vibration analysis of chiral single-walled carbon nanotubes", *Physica E: Low-dimens. Syst. Nanostr.*, **59**, 186-191

Bounouara, F., Benrahou, K.H., Belkorissat, I. and Tounsi, A. (2016), "A nonlocal zeroth-order shear deformation theory for free vibration of functionally graded nanoscale plates resting on elastic foundation", *Steel Compos. Struct.*, **20**(2), 227-249.

Bourada, M., Kaci, A., Houari, M.S.A. and Tounsi, A. (2015), "A new simple shear and normal deformations theory for functionally graded beams", *Steel Compos. Struct.*, **18**(2), 409-423.

Daouadji, T.H., Hadji, L., Meziane, M.A.A. and Bekki, H. (2016), "Elastic analysis effect of adhesive layer characteristics in steel beam strengthened with a fiber-reinforced polymer plates", *Struct. Eng. Mech.*,

59(1), 83-100.
El Mahi, Benrahou, K.H. Belakhdar, Kh., Tounsi, A. and Adda Bedia, El A. (2014), "Effect of the tapered of the end of a FRP plate on the interfacial stresses in a strengthened beam used in civil engineering applications", *Mech. Compos. Mater.*, **50**(4), 465-474.
Guenaneche, B., Tounsi, A. and Adda Bedia, E.A. (2014), "Effect of shear deformation on interfacial stress analysis in plated beams under arbitrary loading", *Adhes. Adhesiv.*, **48**, 1-13.
Hassaine Daouadji, T. and Adim, B. (2015), "Theoretical analysis of composite beams under uniformly distributed load", *Adv. Mater. Res.*, **5**(1), 1-9.
Hassaine Daouadji, T., Abdelaziz, H.H., Tounsi, A. and Adda bedia, E.A. (2013), "Elasticity solution of a cantilever functionally graded beam", *Appl. Compos. Mater.*, **20**(1), 1-15
Hassaine Daouadji, T., Rabahi, A., Abbes, B. and Adim, B. (2016), "Theoretical and finite element studies of interfacial stresses in reinforced concrete beams strengthened by externally FRP laminates plate", *J. Adhes. Sci. Tech.*, **30**(12), 1253-1280.
Krour, B., Bernard, F. and Tounsi, A. (2014), "Fibers orientation optimization for concrete beam strengthened with a CFRP bonded plate: A coupled analytical-numerical investigation", *Eng. Struct.*, **56**, 218-227.
Mori, T. and Tanaka, K. (1973), "Average stress in matrix and average elastic energy of materials with misfitting inclusions", *Acta Metall*, **21**, 571-4.
Rabahi A., Hassaine Daouadji, T., Abbes, B. and Adim, B. (2015), "Analytical and numerical solution of the interfacial stress in reinforced-concrete beams reinforced with bonded prestressed composite plate", *J. Reinf. Plast. Compos.*, **35**(3), 258-272.
Rabahi, A., Adim, B., Chergui, S. and Hassaine Daouadji, T. (2015), "Interfacial stresses in FRP-plated RC beams: effect of adherend shear deformations", *Multiphys. Model. Simul. Syst. Des. Monit. Appl. Condit. Monit.*, **2**, 317-326.
Roberts, T.M. (1989), "Approximate analysis of shear and normal stress concentrations in the adhesive layer of plated RC beams", *Struct. Eng.*, **67**(12), 229-33.
Shen, H.S.,Teng, J.G. and Yang, J. (2001), "Interfacial stresses in beams and slabs bonded with thin plate", *J. Eng. Mech*., ASCE, **127**(4), 399-406.
Smith, S.T. and Teng, J.G. (2001), "Interfacial stresses in plated beams", *Eng. Struct*., **23**(7), 857-71.
Touati, M., Tounsi, A. and Benguediab, M. (2015), "Effect of shear deformation on adhesive stresses in plated concrete beams: Analytical solutions", *Comput. Concrete*, **15**(3), 141-166.
Tounsi, A. (2006), "Improved theoretical solution for interfacial stresses in concrete beams strengthened with FRP plate", *Int. J. Solid. Struct*., **43**, 4154-74.
Tounsi, A., Hassaine Daouadji, T., Benyoucef, S. and Adda bedia, E.A. (2008), "Interfacial stresses in FRP-plated RC beams: Effect of adherend shear deformations", *Int. J. Adhes. Adhesiv.*, **29**(4), 343-351.
Wattanasakulpong, N. and Ungbhakorn, V. (2014), "Linear and nonlinear vibration analysis of elastically restrained ends FGM beams with porosities", *Aerosp. Sci. Tech.*, **32**(1), 111-120.
Yang, J. and Wu, Y.F. (2007), "Interfacial stresses of FRP strengthened concrete beams: Effect of shear deformation", *Compos. Struct.*, **80**, 343-351.
Yang, J. and Ye, J. (2010), "An improved closed-form solution to interfacial stresses in plated beams using a two-stage approach", *Int. J. Mech. Sci.*, **52**, 13-30.
Yang, J., Ye, J. and Niu, Z. (2007), "Interfacial shear stress in FRP-plated RC beams under symmetric loads", *Cement Concrete Compos.*, **29**, 421-432.
Zidani, M.B., Belakhdar, K., Tounsi, A.and Adda Bedia, E.A. (2015), "Finite element analysis of initially damaged beams repaired with FRP plates", *Compos. Struct.*, **134**, 429-439.
Zidour, M., Hassaine Daouadji, T., Benrahou, K.H., Tounsi, A., Bedia, E.A.A. and Hadji, L. (2014), "Buckling analysis of chiral single-walled carbon nanotubes by using the nonlocal Timoshenko beam theory", *Mech. Compos. Mater.*, **50**(1), 95-104